16

Magnetically Nonlinear Dynamic Models of Synchronous Machines: Their Derivation, Parameters and Applications

Gorazd Štumberger[1], Bojan Štumberger[1], Tine Marčič[2]
Miralem Hadžiselimović[1] and Drago Dolinar[1]
[1]*University of Maribor, Faculty of Electrical Engineering and Computer Science*
[2]*TECES- Research and Development Centre of Electrical Machines*
[1,2]*Slovenia*

1. Introduction

This chapter deals with the magnetically nonlinear dynamic models of synchronous machines. More precisely, the chapter focuses on the dynamic models of the permanent magnet synchronous machines and reluctance synchronous machines. A general procedure, which can be applied to derive such magnetically nonlinear dynamic models, is presented. The model is of no use until its parameters are determined. Therefore, some available experimental methods, that are appropriate for determining parameters of the discussed models, are presented. The examples given at the end of the chapter show, how the magnetically nonlinear dynamic models of discussed synchronous machines can be applied.
Generally, in all synchronous machines the resultant magneto-motive force and the rotor move with the same speed. This condition is fulfilled completely only in the case of steady-state operation. However, during the transient operation, the relative speed between the resultant magneto-motive force and the rotor can change. In the case of permanent magnet synchronous machines, the force or torque that causes motion appears due to the interaction between the magnetic fields caused by the permanent magnets and the magnetic excitation caused by the stator currents. On the contrary, in the reluctance synchronous machines the origin of motion is the force or torque caused by the differences in reluctance. Most of the modern permanent magnet synchronous machines utilize both phenomena for the thrust or torque production.
A concise historic overview of the development in the field of synchronous machine modelling, related mostly to the machines used for power generation, is given in (Owen, 1999). When it comes to the modern modelling of electric machines, extremely important, but often neglected, work of Gabriel Kron must be mentioned. In the years from 1935 to 1938, he published in General Electric Review series of papers entitled ``The application of tensors to the analysis of rotating electrical machinery.'' With these publications as well as with (Kron, 1951, 1959, 1965), Kron joined all, at that time available and up to date knowledge, in the fields of physics, mathematics and electric machinery. In such way, he set a solid theoretical background for modern modelling of electric machines. Unfortunately, the generality of Kron's approach faded over time. In modern books related to the modelling and control of

electric machines, such as (Fitzgerald & Kingslley, 1961), (Krause et al., 2002), (Vas, 1992, 2001), (Boldea & Tutelea, 2010), (Jadrić & Frančić, 1997), and (Dolinar & Štumberger, 2006), the tensors proposed by Kron are replaced with matrices. The electric machines are treated as magnetically linear systems, whereas the magnetically nonlinear behaviour of the magnetic cores, which are substantial parts of electric machines, is neglected.

The agreement between measured responses and the ones calculated with the dynamic model of an electric machine cannot be satisfying if magnetically nonlinear behaviour of the magnetic core is neglected. Moreover, if such a model is applied in the control design, the performances of the closed-loop controlled system cannot be superb. In order to improve the agreement between the measured and calculated responses of electric machines and to improve performances of the closed-loop controlled systems, individual authors make an attempt to include the magnetically nonlinear behaviour of magnetic cores into dynamic models of electric machines.

In the research field of synchronous machines, the effects of saturation are considered by the constant saliency ratio and variable inductance (Iglesias, 1992), (Levi & Levi, 2000), (Vas, 1986). In (Tahan, & Kamwa, 1995), the authors apply two parameters to describe the magnetically nonlinear behaviour of the magnetic core of a synchronous machine. The authors in (Štumberger B. et al., 2003) clearly show that only one parameter is insufficient to properly describe magnetically nonlinear behaviour of a permanent magnet synchronous machine. A magnetically nonlinear and anisotropic magnetic core model of a synchronous reluctance machine, based on current dependent flux linkages, is presented in (Štumberger G. et al., 2003). The constraints that must be fulfilled in the conservative or loss-less magnetic core model of any electric machine are given in (Melkebeek & Willems, 1990) and (Sauer, 1992). A new, energy functions based, magnetically nonlinear model of a synchronous reluctance machine is proposed in (Vagati et al., 2000), while the application of this model in the sensorless control is shown in (Capecchi et al., 2001) and (Guglielmi et al., 2006). One of the first laboratory realizations of the nonlinear input-output linearizing control, considering magnetic saturation in the induction machine, is presented in (Dolinar et al., 2003). Similar approach is applied in the case of linear synchronous reluctance machine in (Dolinar et al., 2005). The design of this machine is presented in (Hamler et al., 1998), whereas the magnetically nonlinear model of the magnetic core, given in the form of current and position dependent flux linkages, is presented in (Štumberger et al., 2004a). Further development of the magnetically nonlinear dynamic model of synchronous reluctance machine, based on the current and position dependent flux linkages expressed with Fourier series, is presented in (Štumberger et al., 2006). An extension to the approach presented in (Štumberger et al., 2004a, 2004b, 2006) towards the magnetically nonlinear dynamic models of permanent magnet synchronous machines is made in (Hadžiselimović, 2007a), (Hadžiselimović et al., 2007b, 2008), where the impact of permanent magnets is considered as well.

The experimental methods appropriate for determining parameters of the magnetically nonlinear dynamic model of a linear synchronous reluctance motor are presented in (Štumberger et al., 2004b). They are based on the stepwise changing voltages generated by a voltage source inverter controlled in the *d-q* reference frame. Quite different method for determining parameters of the synchronous machines, based on the supply with sinusoidal voltages, is proposed in (Rahman & Hiti, 2005). A set of experimental methods, appropriate for determining the magnetically nonlinear characteristics of electromagnetic devices and electric machines with magnetic cores, is presented in (Štumberger et al., 2005). However,

the methods presented in (Štumberger et al., 2005) could fail when damping windings are wound around the magnetic core, which is solved by the methods proposed in (Štumberger et al., 2008b). In the cases, when the test required in the experimental methods cannot be performed on the electric machine, the optimization based methods, like those presented in (Štumberger et al., 2008a) and (Marčič et al., 2008), can be applied for determining parameters required in the magnetically nonlinear dynamic models.

Many authors use magnetically nonlinear dynamic models of synchronous machines. However, it is often not explained how the models are derived and how their parameters are determined. In the section 2, the three-phase model of a permanent magnet synchronous machine with reluctance magnetic core is written in a general form. The effects of saturation, cross-saturation as well as the interactions between the permanent magnets and slots are considered by the current and position dependent characteristics of flux linkages. Since only those dynamic models with independent state variables are appropriate for the control design, the two-axis magnetically nonlinear dynamic model written in the *d-q* reference frame is derived. The derived model of the permanent magnet synchronous machine is simplified to the model of a synchronous reluctance machine, which is further modified to the model of a linear synchronous reluctance machine. The experimental methods appropriate for determining parameters, that are required in the magnetically nonlinear dynamic models, are presented in the section 3. The performance of the magnetically nonlinear dynamic model as well as applications of the models is shown in the section 4. The chapter ends with the conclusion given in the section 5 and references given in the section 6.

2. Derivation of the magnetically nonlinear dynamic model

The magnetically nonlinear properties of the ferromagnetic material are normally described in the form of $B(H)$ characteristics, defined with the magnetic flux density B and the magnetic field strength H (Boll, 1990). These characteristics can be determined by different tests and measurements performed on a material specimen (Abdallh, 2009). In the case of an isotropic material, the properties changing along the hysteresis loop can be described by the differential permeability defined with the partial derivative $\partial B/\partial H$. However, in the case of an anisotropic material, the local relations between the flux density vector $\mathbf{B}$ and the magnetic field strength vector $\mathbf{H}$ are given in the form of the differential permeability tensor, defined with the partial derivative $\partial\mathbf{B}/\partial\mathbf{H}$.

An electric machine or an electromagnetic device consists at least from a magnetic core and windings wound around the core, which means that the materials with different properties are combined. Thus, the magnetically nonlinear behaviour of the entire electric machine or electromagnetic device is influenced by different materials. This influence is present also in the variables measured on the terminals of the machine. The time behaviour of the variables measured on the terminals can be used to describe the magnetically nonlinear behaviour of the machine. In the case of an electric machine with only one winding, the magnetically nonlinear behaviour of the machine can be described in the form of the $\psi(i)$ characteristic, where the flux linkage ψ and the current i can be determined with the measurement of currents and voltages on the terminals of the machine. Similarly as in the case of $B(H)$ characteristic, the local behaviour along the $\psi(i)$ characteristic can be described with the partial derivative $\partial\psi/\partial i$. However, when more than one winding is wound around the common magnetic core, the flux linkages and currents of individual windings can be used to compose the flux linkage vector $\boldsymbol{\psi}$ and the current vector $\mathbf{i}$. Again, the partial derivative $\partial\boldsymbol{\psi}/\partial\mathbf{i}$ can be used to describe the locally

nonlinear behaviour of the magnetic core. It is wise to compose the flux linkage vector and the current vector from the linearly independent variables.

2.1 Permanent magnet synchronous machine

The derivation performed in this subsection is given for the two-pole, three-phase permanent magnet synchronous machine (Hadžiselimović, 2007a), (Hadžiselimović et al., 2007b, 2008). It is schematically shown in Fig. 1. The axes *a*, *b* and *c* are defined with the magnetic axes of the phase *a*, *b* and *c* windings.

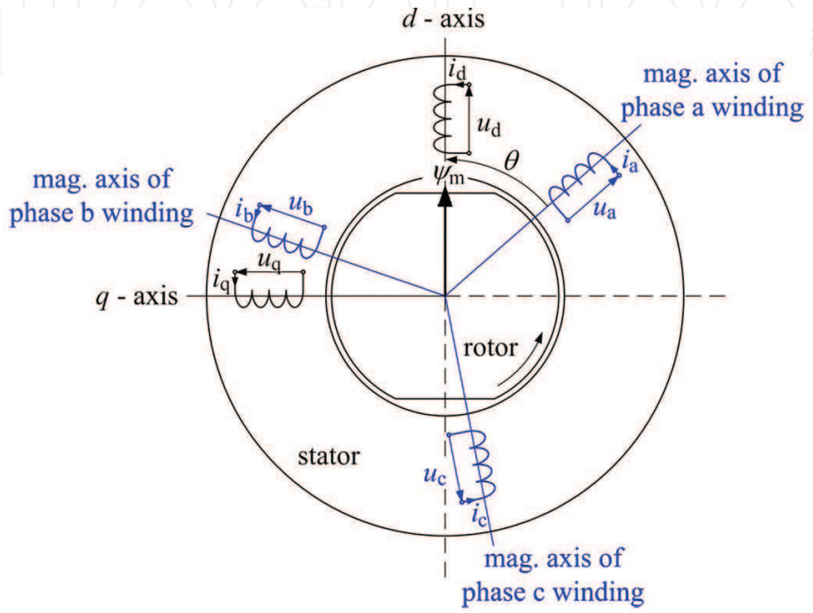

Fig. 1. Schematic presentation of a two-pole, three-phase permanent magnet synchronous machine

The model windings shown in Fig. 1 are aligned with the magnetic axes of the actual phase windings, whereas the effect of the permanent magnets is considered through the flux linkage vector $\boldsymbol{\psi}_m$ with the length ψ_m. The *d*-axis is aligned with the flux linkage vector and, the *q*-axis is displaced by an electric angle of $\pi/2$. Since the permanent magnets are located on the rotor, the angle θ represents the rotor position or the displacement of the *d*-axis with respect to the phase *a* magnetic axis. The magnetic axes of the phase *a*, *b* and *c* windings are treated as the reference frame *abc*. The voltage balances in the individual phase windings of the machine shown in Fig. 1 are described by (1) and (2):

$$\mathbf{u}_{abc} = \mathbf{R}\mathbf{i}_{abc} + \frac{d}{dt}\boldsymbol{\psi}_{abc} + \frac{d}{dt}\boldsymbol{\psi}_{mabc} \tag{1}$$

$$\mathbf{u}_{abc} = \begin{bmatrix} u_a \\ u_b \\ u_c \end{bmatrix};\ \mathbf{i}_{abc} = \begin{bmatrix} i_a \\ i_b \\ i_c \end{bmatrix};\ \boldsymbol{\psi}_{abc} = \begin{bmatrix} \psi_a(i_a, i_b, i_c, \theta) \\ \psi_b(i_a, i_b, i_c, \theta) \\ \psi_c(i_a, i_b, i_c, \theta) \end{bmatrix};\ \boldsymbol{\psi}_{mabc} = \begin{bmatrix} \psi_{ma}(\theta) \\ \psi_{mb}(\theta) \\ \psi_{mc}(\theta) \end{bmatrix};\ \mathbf{R} = \begin{bmatrix} R_a & & \\ & R_b & \\ & & R_c \end{bmatrix} \tag{2}$$

where $k \in \{a,b,c\}$ denotes the three phases, u_k, i_k, and R_k are the phase *k* voltage, current, and resistance, respectively. ψ_k is the phase *k* flux linkages due to the stator current excitation,

while ψ_{mk} is the phase k flux linkages due to the permanent magnets. The flux linkages caused by the stator current excitation are treated as position and current dependent $\psi_k(i_a,i_b,i_c,\theta)$, whereas the flux linkages caused by the permanent magnets are treated as position dependent $\psi_{mk}(\theta)$. In such way, the impact of the stator currents on the flux linkages, caused by the permanent magnets, is neglected. The equations (1) and (2) are completed by (3) describing motion:

$$J\frac{d^2\theta}{dt^2} = t_e(i_a,i_b,i_c,\psi_m,\theta) - t_l - b\frac{d\theta}{dt} \tag{3}$$

where J is the moment of inertia, t_e is the electric torque, t_l is the load torque, b is the coefficient of the viscous friction, while $\omega = d\theta/dt$ is the angular speed. The effects of slotting, saturation and cross-saturation as well as the effects, caused by the interactions between the permanent magnets and slots, are included in the model with the current and position dependent characteristics of flux linkages and electric torque. They can be determined either experimentally or by applying some of the numerical methods, like finite element method. When the resistances and characteristics of the flux linkages and electric torque are known, the model can be applied for calculation of different transient and steady-state conditions. Unfortunately, the electric machines used in the controlled drives are mostly wye-connected, which means that the sum of all three currents equals zero. Thus, the state variables of the proposed model, given by (1) to (3), are linearly dependent, which causes algebraic loops and problems with convergence during simulations. Moreover, only the dynamic models with independent state variables can be used for the control synthesis. It seems that all the aforementioned effects are considered in the model given by (1) to (3), however, the model itself is useless. The question is: how the model should be modified to become useful?

One of the possibilities is the reduction of dependent state and input variables. In this case, the model should be described using only two independent currents and only two independent line to line voltages. Another possibility is the transformation of the model into the *d-q* reference frame, which is a common approach in the case of magnetically linear models. According to (Fitzgerald et al., 1961) and (Krause et al., 2002), this transformation can be performed exclusively for the magnetically linear models, which is true. However, it is also true, that not the model, but its variables, can be transformed into any arbitrary reference frame, if the inverse transformation exists whereas the variables can be written in a unique way in the new reference frame. According to Fig. 1, the relations between the axes *a*, *b* and *c*, which define the reference frame *abc*, and the *d*-axis, *q*-axis and *0*-axis, which define the reference frame *dq0*, are described by the transformation matrix **T** (4):

$$\mathbf{T} = \sqrt{\frac{2}{3}}\begin{bmatrix} \cos(\theta) & -\sin(\theta) & 1/\sqrt{2} \\ \cos\left(\theta + 4/3\,\pi\right) & -\sin\left(\theta + 4/3\,\pi\right) & 1/\sqrt{2} \\ \cos\left(\theta + 2/3\,\pi\right) & -\sin\left(\theta + 2/3\,\pi\right) & 1/\sqrt{2} \end{bmatrix} \tag{4}$$

where the *0*-axis, not shown in Fig. 1, is orthogonal to the *d*-axis and *q*-axis. The transformation matrix **T** is orthogonal, which means that the inverse matrix equals the transposed original matrix $\mathbf{T}^{-1}=\mathbf{T}^{T}$. Moreover, the orthogonal transformation matrix assures the invariance of power.

Let us express the voltages, currents and flux linkages, written in the *abc* reference frame in (2), with the transformation matrix and voltages, currents and flux linkages written in the *dq0* reference frame (5), (6).

$$\mathbf{u}_{abc} = \mathbf{T}\mathbf{u}_{dq0};\ \ \mathbf{i}_{abc} = \mathbf{T}\mathbf{i}_{dq0};\ \ \ \boldsymbol{\psi}_{mabc} = \mathbf{T}\boldsymbol{\psi}_{mdq0};\ \ \ \boldsymbol{\psi}_{abc} = \mathbf{T}\boldsymbol{\psi}_{dq0}; \tag{5}$$

$$\mathbf{u}_{dq0} = \begin{bmatrix} u_d \\ u_q \\ u_0 \end{bmatrix};\ \mathbf{i}_{dq0} = \begin{bmatrix} i_d \\ i_q \\ i_0 \end{bmatrix};\ \boldsymbol{\psi}_{dq0} = \begin{bmatrix} \psi_d(i_d, i_q, i_0, \theta) \\ \psi_q(i_d, i_q, i_0, \theta) \\ \psi_0(i_d, i_q, i_0, \theta) \end{bmatrix};\ \boldsymbol{\psi}_{mdq0} = \begin{bmatrix} \psi_{md}(\theta) \\ \psi_{mq}(\theta) \\ \psi_{m0}(\theta) \end{bmatrix} \tag{6}$$

By inserting (5) into (1), equations (7) to (10) are obtained.

$$\mathbf{T}\mathbf{u}_{dq0} = \mathbf{R}\mathbf{T}\mathbf{i}_{dq0} + \frac{d}{dt}\left\{\mathbf{T}\boldsymbol{\psi}_{dq0}\right\} + \frac{d}{dt}\left\{\mathbf{T}\boldsymbol{\psi}_{mdq0}\right\} \tag{7}$$

$$\mathbf{u}_{dq0} = \mathbf{T}^{-1}\mathbf{R}\mathbf{T}\mathbf{i}_{dq0} + \mathbf{T}^{-1}\frac{d}{dt}\left\{\mathbf{T}\boldsymbol{\psi}_{dq0}\right\} + \mathbf{T}^{-1}\frac{d}{dt}\left\{\mathbf{T}\boldsymbol{\psi}_{mdq0}\right\} \tag{8}$$

$$\mathbf{u}_{dq0} = \mathbf{T}^{-1}\mathbf{R}\mathbf{T}\mathbf{i}_{dq0} + \mathbf{T}^{-1}\frac{d}{dt}\{\mathbf{T}\}\boldsymbol{\psi}_{dq0} + \mathbf{T}^{-1}\mathbf{T}\frac{d}{dt}\left\{\boldsymbol{\psi}_{dq0}\right\} + \mathbf{T}^{-1}\frac{d}{dt}\{\mathbf{T}\}\boldsymbol{\psi}_{mdq0} + \mathbf{T}^{-1}\mathbf{T}\frac{d}{dt}\left\{\boldsymbol{\psi}_{mdq0}\right\} \tag{9}$$

$$\mathbf{u}_{dq0} = \mathbf{T}^{-1}\mathbf{R}\mathbf{T}\mathbf{i}_{dq0} + \mathbf{T}^{-1}\frac{d}{dt}\{\mathbf{T}\}\boldsymbol{\psi}_{dq0} + \frac{d}{dt}\left\{\boldsymbol{\psi}_{dq0}\right\} + \mathbf{T}^{-1}\frac{d}{dt}\{\mathbf{T}\}\boldsymbol{\psi}_{mdq0} + \frac{d}{dt}\left\{\boldsymbol{\psi}_{mdq0}\right\} \tag{10}$$

After considering (4) and (6) in (10), the voltage equation (11) is obtained:

$$\begin{bmatrix} u_d \\ u_q \\ u_0 \end{bmatrix} = R\begin{bmatrix} i_d \\ i_q \\ i_0 \end{bmatrix} + \begin{bmatrix} \frac{\partial\psi_d}{\partial i_d} & \frac{\partial\psi_d}{\partial i_q} & \frac{\partial\psi_d}{\partial i_0} \\ \frac{\partial\psi_q}{\partial i_d} & \frac{\partial\psi_q}{\partial i_q} & \frac{\partial\psi_q}{\partial i_0} \\ \frac{\partial\psi_0}{\partial i_d} & \frac{\partial\psi_0}{\partial i_q} & \frac{\partial\psi_0}{\partial i_0} \end{bmatrix}\frac{d}{dt}\begin{bmatrix} i_d \\ i_q \\ i_0 \end{bmatrix} + \frac{d\theta}{dt}\left\{\begin{bmatrix} \frac{\partial\psi_d}{\partial\theta} \\ \frac{\partial\psi_q}{\partial\theta} \\ \frac{\partial\psi_0}{\partial\theta} \end{bmatrix} + \begin{bmatrix} -\psi_q \\ \psi_d \\ 0 \end{bmatrix} + \begin{bmatrix} \frac{\partial\psi_{md}}{\partial\theta} \\ \frac{\partial\psi_{mq}}{\partial\theta} \\ \frac{\partial\psi_{m0}}{\partial\theta} \end{bmatrix} + \begin{bmatrix} -\psi_{mq} \\ \psi_{md} \\ 0 \end{bmatrix}\right\} \tag{11}$$

where $R=R_a=R_b=R_c$ denotes the stator resistance. It must be explained that after performing similar derivation for the magnetically liner dynamic model in (Fitzgerald et al., 1961) and (Krause et al., 2002), the model written in the *dq0* reference frame is obtained together with the model parameters. However, in the case of magnetically nonlinear model, treated in this chapter, only the form of the matrix voltage equation is obtained. The model is of no use until the characteristics of flux linkages in the *dq0* reference frame are determined. To carry out this, a voltage source inverter controlled in the *dq0* reference frame can be applied.

Due to the wye connected winding, the sum of currents i_a, i_b and i_c equals zero, whereas considering the transformation matrix **T** (4), (5) and (6) yields (12).

$$i_a + i_b + i_c = 0 \quad \Rightarrow \quad i_0 = \sqrt{\frac{2}{3}}\frac{1}{\sqrt{2}}\left(i_a + i_b + i_c\right) = 0 \tag{12}$$

Thus, the current in the neutral conductor i_0 equals 0. The neutral point voltage u_0 appears due to the changing flux linkages ψ_0 and ψ_{m0} which are caused by the changing level of the saturation in individual parts of the machine. The flux linkage ψ_0 is caused by the current excitation and the flux linkage ψ_{m0} appears due to the permanent magnets. When the discussed machine is closed-loop current controlled, the current controllers implicitly compensate u_0. Thus, the neutral conductor current i_0 and the neutral point voltage u_0 equal zero. They are caused by the changing flux linkages ψ_0 and ψ_{m0}, which influence only on u_0 and i_0, and are not coupled with the d-axis or q-axis components. Therefore, in the case of closed-loop current controlled machine, the zero component voltage, current and flux linkages in (11) can be neglected, which leads to the voltage equation (13).

$$\begin{bmatrix} u_d \\ u_q \end{bmatrix} = R\begin{bmatrix} i_d \\ i_q \end{bmatrix} + \begin{bmatrix} \frac{\partial \psi_d}{\partial i_d} & \frac{\partial \psi_d}{\partial i_q} \\ \frac{\partial \psi_q}{\partial i_d} & \frac{\partial \psi_q}{\partial i_q} \end{bmatrix} \frac{d}{dt}\begin{bmatrix} i_d \\ i_q \end{bmatrix} + \frac{d\theta}{dt}\left\{ \begin{bmatrix} \frac{\partial \psi_d}{\partial \theta} \\ \frac{\partial \psi_q}{\partial \theta} \end{bmatrix} + \begin{bmatrix} -\psi_q \\ \psi_d \end{bmatrix} + \begin{bmatrix} \frac{\partial \psi_{md}}{\partial \theta} \\ \frac{\partial \psi_{mq}}{\partial \theta} \end{bmatrix} + \begin{bmatrix} -\psi_{mq} \\ \psi_{md} \end{bmatrix} \right\} \tag{13}$$

Thus, the $dq0$ reference frame is reduced to the dq reference frame. In order to complete the magnetically nonlinear dynamic model of the permanent magnet synchronous machine, the torque expression in (3) must be written in the dq reference frame too. According to (Krause et al., 2002), in the cases of magnetically nonlinear magnetic core, the co-energy approach can be used to determine the torque expression. Since the co-energy approach is rather demanding, another approach, which is often used in the machine design, is applied in this section. It gives very good results in the case of surface permanent magnet machines whereas in the other cases, it normally represents an acceptable approximation. If the leakage flux linkages are neglected and the energy in the magnetic field due to the permanent magnets is considered as constant, the back electromotive forces multiplied by the corresponding currents represent the mechanical power at the shaft of the machine $d\theta/dt\ t_e$ (14).

$$\frac{d\theta}{dt} t_e = e_d i_d + e_q i_q = \frac{d\theta}{dt}\left(\frac{\partial \psi_d}{\partial \theta} + \frac{\partial \psi_{md}}{\partial \theta} - \psi_q - \psi_{mq} \right) i_d + \frac{d\theta}{dt}\left(\frac{\partial \psi_q}{\partial \theta} + \frac{\partial \psi_{mq}}{\partial \theta} + \psi_d + \psi_{md} \right) i_q \tag{14}$$

With the comparison of the left hand side and the right hand side of (14), the electric torque can be expressed by (15):

$$t_e = \left(\frac{\partial \psi_d}{\partial \theta} + \frac{\partial \psi_{md}}{\partial \theta} - \psi_q - \psi_{mq} \right) i_d + \left(\frac{\partial \psi_q}{\partial \theta} + \frac{\partial \psi_{mq}}{\partial \theta} + \psi_d + \psi_{md} \right) i_q \tag{15}$$

which represents the torque equation of a two-pole synchronous permanent magnet machine. By neglecting the partial derivatives in (15), the effects of slotting and the effects of interactions between the slots and permanent magnets are neglected. By neglecting additionally the terms ψ_d, ψ_q, and ψ_{mq}, (15) reduces to the well known torque expression of a permanent magnet synchronous machine (Krause et al., 2002).

The magnetically nonlinear two-axis dynamic model of a two-pole permanent magnet synchronous machine, written in the dq reference frame, is given in its final form by the voltage equation (13), the torque equation (15) and the equation describing motion (16).

$$J\frac{d^2\theta}{dt^2} = t_e - t_l - b\frac{d\theta}{dt} \tag{16}$$

The current and position dependent characteristics of flux linkages $\psi_d(i_d,i_q,\theta)$ and $\psi_q(i_d,i_q,\theta)$, caused by the current excitation, as well as the position dependent characteristics of flux linkages $\psi_{md}(\theta)$ and $\psi_{mq}(\theta)$, caused by the permanent magnets, are applied in the model. They are used to account for the effects of saturation and cross-saturation, the effects of slotting and the effects caused by the interactions between the permanent magnets and slots.

2.2 Reluctance synchronous machine

The magnetically nonlinear dynamic model of a synchronous reluctance machine (Štumberger G. et al., 2003, 2004a, 2004b) can be derived from the model of the permanent magnet synchronous machine, by neglecting all the terms related with the permanent magnets. Thus, all the terms containing ψ_{md} and ψ_{mq} in (13) and (15) are dropped out. Only the flux linkages caused by the current excitation appear in the equations. In the case of the reluctance motor, the flux linkage vector due to the permanent magnets is missing. Therefore, the d-axis and the q-axis are defined with the directions of the minimum and the maximum reluctance, respectively. Both axes are displaced by the electric angle of $\pi/2$. In such way, the two-axis magnetically nonlinear dynamic model of the two-pole, three-phase synchronous reluctance machine is obtained. It is given by the voltage equation (17), the torque equation (18) and the equation describing motion (19).

$$\begin{bmatrix} u_d \\ u_q \end{bmatrix} = R\begin{bmatrix} i_d \\ i_q \end{bmatrix} + \begin{bmatrix} \frac{\partial\psi_d}{\partial i_d} & \frac{\partial\psi_d}{\partial i_q} \\ \frac{\partial\psi_q}{\partial i_d} & \frac{\partial\psi_q}{\partial i_q} \end{bmatrix}\frac{d}{dt}\begin{bmatrix} i_d \\ i_q \end{bmatrix} + \frac{d\theta}{dt}\left\{\begin{bmatrix} \frac{\partial\psi_d}{\partial\theta} \\ \frac{\partial\psi_q}{\partial\theta} \end{bmatrix} + \begin{bmatrix} -\psi_q \\ \psi_d \end{bmatrix}\right\} \tag{17}$$

$$t_e = \left(\frac{\partial\psi_d}{\partial\theta} - \psi_q\right)i_d + \left(\frac{\partial\psi_q}{\partial\theta} + \psi_d\right)i_q \tag{18}$$

$$J\frac{d^2\theta}{dt^2} = t_e - t_l - b\frac{d\theta}{dt} \tag{19}$$

The effects of slotting, saturation, and cross-saturation are considered in the model by the current and position dependent characteristics of flux linkages.

2.3 Linear reluctance synchronous machine

The dynamic model of the rotary synchronous reluctance machine, given by (17) to (19) must be modified, to be suitable for appropriate description of the dynamic conditions in the linear synchronous reluctance machine (LSRM) (Štumberger G. et al., 2003, 2004a, 2004b). The design of this machine is described in (Hamler et al. 1998), whereas similar machines are described in (Daldaban & Ustkoyuncu, 2006, 2007, 2010). It has a short and moving primary called mover and a long reluctance secondary. It is supplied from the primary where windings are placed. The LSRM, schematically presented in Fig. 2, performs translational motion.

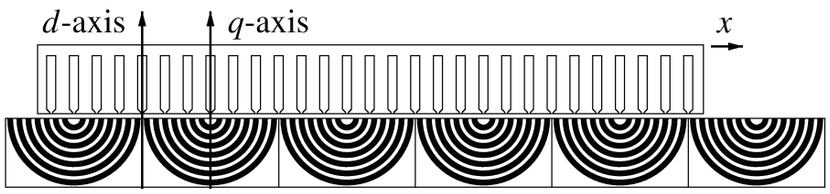

Fig. 2. Schematic presentation of a linear synchronous reluctance machine

In (17) to (19), the angular position θ is expressed with the position x and the pole pitch τ_p (20).

$$\theta = \frac{\pi}{\tau_p} x \tag{20}$$

This leads to changes in (19), where the moment of inertia J is replaced with the mass of the mover m, while the electric torque t_e and the load torque t_l are replaced with the thrust F_e and the load force F_l. The obtained magnetically nonlinear dynamic model of the linear synchronous reluctance machine is given by (21) to (23), where F_f is the friction force.

$$\begin{bmatrix} u_d \\ u_q \end{bmatrix} = R \begin{bmatrix} i_d \\ i_q \end{bmatrix} + \begin{bmatrix} \frac{\partial \psi_d}{\partial i_d} & \frac{\partial \psi_d}{\partial i_q} \\ \frac{\partial \psi_q}{\partial i_d} & \frac{\partial \psi_q}{\partial i_q} \end{bmatrix} \frac{d}{dt} \begin{bmatrix} i_d \\ i_q \end{bmatrix} + \frac{\pi}{\tau_p} \frac{dx}{dt} \left\{ \begin{bmatrix} \frac{\partial \psi_d}{\partial x} \\ \frac{\partial \psi_q}{\partial x} \end{bmatrix} + \begin{bmatrix} -\psi_q \\ \psi_d \end{bmatrix} \right\} \tag{21}$$

$$t_e = \frac{\pi}{\tau_p} \left(\psi_d i_q - \psi_q i_d \right) + \frac{\partial \psi_d}{\partial x} i_d + \frac{\partial \psi_q}{\partial x} i_q \tag{22}$$

$$m \frac{d^2 x}{dt^2} = F_e - F_l - F_f \tag{23}$$

In the case of linear synchronous reluctance motor, the current and position dependent characteristics of flux linkages are used to consider not only the effects of slotting, saturation and cross-saturation, but also the end effects. The end effects appear only in the linear machines due to the finite lengths of the primary and secondary. In linear machines, the end-poles and the windings in these poles cannot be symmetrical. On the contrary, in the rotational machines the stator and rotor are cylindrical and closed in themselves. The path along the circumference of the stator or rotor apparently never ends, whereas all the poles and phase windings are symmetrical.

For the given constant values of the currents i_d and i_q, the position dependent flux linkages ψ_d and ψ_q can be expressed in the form of Fourier series (24) and (25):

$$\psi_d = \psi_{d0} + \sum_{h=1}^{N} \left(\psi_{dch} \cos(\frac{\pi}{\tau_p} hx) + \psi_{dsh} \sin(\frac{\pi}{\tau_p} hx) \right) \tag{24}$$

$$\psi_q = \psi_{q0} + \sum_{h=1}^{N} \left(\psi_{qch} \cos(\frac{\pi}{\tau_p} hx) + \psi_{qsh} \sin(\frac{\pi}{\tau_p} hx) \right) \tag{25}$$

where N is the number of considered higher order harmonics, h denotes the harmonic order while ψ_{d0}, ψ_{dch}, ψ_{dsh} and ψ_{q0}, ψ_{qch}, ψ_{qsh} are the Fourier coefficients. After inserting (24) and (25) into (22), the position dependent thrust $F_e(x)$ can be expressed by (26):

$$F_e(x) = F_0 + \sum_{h=1}^{N}\left(F_{ch}\cos(\frac{\pi}{\tau_p}hx) + F_{sh}\sin(\frac{\pi}{\tau_p}hx) \right) \tag{26}$$

where F_0, F_{ch} and F_{sh} are the Fourier coefficients. The mean value of the thrust is given by F_0 (27), whereas the position dependent thrust pulsation is described by F_{ch} (28) and F_{sh} (29).

$$F_0 = \frac{\pi}{\tau_p}\left(\psi_{d0}i_q - \psi_{q0}i_d\right) \tag{27}$$

$$F_{ch} = \frac{\pi}{\tau_p}\left(\psi_{dch}i_q - \psi_{qch}i_d + h\left(\psi_{dsh}i_d + \psi_{qsh}i_q\right)\right) \tag{28}$$

$$F_{sh} = \frac{\pi}{\tau_p}\left(\psi_{dsh}i_q - \psi_{qsh}i_d - h\left(\psi_{dch}i_d + \psi_{qch}i_q\right)\right) \tag{29}$$

The mean value of the thrust, given by F_0 (27), is well known thrust equation of linear synchronous reluctance machines.

All the dynamic models presented in this section can be easily realized in the program packages like Matlab/Simulink. However, they are of no use without model parameters, given in the form of current and position dependent characteristics of flux linkages. They can be easily implemented in the models using the multi-dimensional lookup tables.

3. Determining dynamic model parameters

The magnetically nonlinear dynamic models of synchronous machines presented in the section 2 are of no use until the model parameters are determined in the form of current and position dependent characteristics of flux linkages. In the subsection 3.1, the experimental method appropriate for determining the position dependent characteristics of flux linkages due to the permanent magnets is presented (Hadžiselimović et al., 2007b). Similarly, the subsection 3.2 describes the experimental method appropriate for determining the current and position dependent characteristics of flux linkages caused by the current excitation (Štumberger G. et al., 2004b). The experimental methods which can be used to determine the thrust and the friction force characteristics of a linear synchronous reluctance motor are presented in the subsection 3.3 (Štumberger G. et al., 2004b). In order to determine the aforementioned characteristics, a special experimental setup is applied. The tested machine is supplied from a voltage source inverter controlled in the dq reference frame. The closed-loop current control in the one axis is combined with the open-loop voltage control in the other axis.

3.1 Position dependent flux linkages caused by the permanent magnets

The angular position θ dependent characteristcis of flux linkages $\psi_{md}(\theta)$ and $\psi_{mq}(\theta)$, required in (13) and (15), can be determined from the waveforms of the three-phase back electromotive forces e_a, e_b and e_c. They can be measured on the open terminals of the tested permanent magnet synchronous machine, driven by another motor at the constant speed ω

$=d\theta/dt$. Using (4) in (5), the e_a, e_b and e_c are transformed into dq reference frame. In such way, the waveforms of e_d and e_q are determined. Since the machine terminals are open, the currents i_d, i_q and consequently the flux linkages ψ_d, ψ_q, caused by these currents, equal zero. Considering this, (13) is reduced to (30).

$$\frac{e_d}{\omega} = -\psi_{mq} + \frac{\partial \psi_{md}}{\partial \theta}, \qquad \frac{e_q}{\omega} = \psi_{md} + \frac{\partial \psi_{mq}}{\partial \theta} \tag{30}$$

The second partial derivatives of expressions in (30) give (31), whereas after considering (30) in (31), (32) is obtained.

$$\frac{\partial}{\partial \theta}\left(\frac{e_d}{\omega}\right) = -\frac{\partial \psi_{mq}}{\partial \theta} + \frac{\partial^2 \psi_{md}}{\partial \theta^2}, \qquad \frac{\partial}{\partial \theta}\left(\frac{e_q}{\omega}\right) = \frac{\partial \psi_{md}}{\partial \theta} + \frac{\partial^2 \psi_{mq}}{\partial \theta^2} \tag{31}$$

$$\frac{\partial^2 \psi_{md}}{\partial \theta^2} + \psi_{md} = \frac{\partial}{\partial \theta}\left(\frac{e_d}{\omega}\right) + \frac{e_q}{\omega}, \qquad \frac{\partial^2 \psi_{mq}}{\partial \theta^2} + \psi_{mq} = \frac{\partial}{\partial \theta}\left(\frac{e_q}{\omega}\right) - \frac{e_d}{\omega} \tag{32}$$

The known waveforms of e_d and e_q, as well as the unknown flux linkage $\psi_{md}(\theta)$ and $\psi_{mq}(\theta)$, can be represented in the form of Fourier series (33) to (36):

$$e_d = e_{d0} + \sum_{h=1}^{N} \left(e_{dch} \cos(h\theta) + e_{dsh} \sin(h\theta) \right) \tag{33}$$

$$e_q = e_{q0} + \sum_{h=1}^{N} \left(e_{qch} \cos(h\theta) + e_{qsh} \sin(h\theta) \right) \tag{34}$$

$$\psi_{md} = \psi_{md0} + \sum_{h=1}^{N} \left(\psi_{mdch} \cos(h\theta) + \psi_{mdsh} \sin(h\theta) \right) \tag{35}$$

$$\psi_{mq} = \psi_{mq0} + \sum_{h=1}^{N} \left(\psi_{mqch} \cos(h\theta) + \psi_{mqsh} \sin(h\theta) \right) \tag{36}$$

where N is the number of considered higher order harmonics, e_{d0}, e_{dch}, e_{dsh} and e_{q0}, e_{qch}, e_{qsh} are the Fourier coefficients of back electromotive forces, while ψ_{md0}, ψ_{mdch}, ψ_{mdsh} and ψ_{mq0}, ψ_{mqch}, ψ_{mqsh} are the Fourier coefficients of flux linkages. The expressions (33) to (36) are applied to calculate the partial derivatives required in (32). The results are given in (37) and (38) for the harmonic order h. With the comparison of the terms on the left hand side and on the right hand side of equations (37) and (38), the expressions for calculation of ψ_{mdch}, ψ_{mdsh}, ψ_{mqch}, and ψ_{mqsh} are obtained. They are given in (39).

$$\left(1-h^2\right)\left(\psi_{mdch}\cos\left(h\theta\right) + \psi_{mdsh}\sin\left(h\theta\right)\right) = \frac{he_{dsh} + e_{qch}}{\omega}\cos\left(h\theta\right) + \frac{-he_{dch} + e_{qsh}}{\omega}\sin\left(h\theta\right) \tag{37}$$

$$\left(1-h^2\right)\left(\psi_{mqch}\cos\left(h\theta\right) + \psi_{mqsh}\sin\left(h\theta\right)\right) = \frac{he_{qsh} - e_{dch}}{\omega}\cos\left(h\theta\right) + \frac{-he_{qch} - e_{dsh}}{\omega}\sin\left(h\theta\right) \tag{38}$$

$$\psi_{mdch}=\frac{he_{dsh}+e_{qch}}{\left(1-h^2\right)\omega},\quad \psi_{mdsh}=\frac{-he_{dch}+e_{qsh}}{\left(1-h^2\right)\omega},\quad \psi_{mqch}=\frac{he_{qsh}-e_{dch}}{\left(1-h^2\right)\omega},\quad \psi_{mqsh}=\frac{-he_{qch}-e_{dsh}}{\left(1-h^2\right)\omega} \tag{39}$$

More details related to this method can be found in (Hadžiselimović, 2007b), (Hadžiselimović et al., 2007b).

3.2 Current and position dependent flux linkages caused by the current excitation

The characteristics of the current and position dependent flux linkages are determined using the experimental setup schematically presented in Fig. 3.

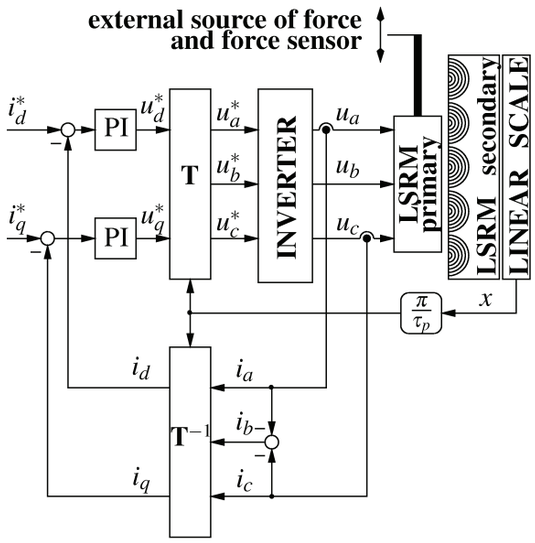

Fig. 3. Schematic presentation of the applied experimental setup

It consists of a tested linear synchronous reluctance machine (LSRM), controlled voltage source inverter, external driving motor used as an external source of force, measurement chains, and control system with digital signal processor (DSP). The DSP is applied to realize the closed-loop current control and the open-loop voltage control in the *dq* reference frame. The PI controllers are used for the closed-loop control, whereas the required transformations are performed using the transformation matrix **T** (4). The reference values in Fig. 3 are marked with *. The inverter, measurement chains, and transformations make possible treatment of the tested three-phase LSRM through its two-axis dynamic model, given by (21) to (23). The current and position measurement chains are used to close the control loops in the applied control algorithm. The force measurements chain is used off-line.

In order to determine the current and position dependent characteristics of flux linkages $\psi_d(i_d,i_q,x)$ and $\psi_q(i_d,i_q,x)$, the mover of the LSRM is locked at the chosen position. The current in one axis is closed-loop controlled in order to maintain the preset constant value, while the voltage in the orthogonal axis is changed in a stepwise manner. Let us suppose that the mover is locked, while the current i_q is closed loop controlled and can be treated as constant. In such conditions, the u_d in (21) can be expressed by (40), which leads to (41).

$$u_d=Ri_d+\frac{\partial\psi_d}{\partial i_d}\frac{di_d}{dt}=Ri_d+\frac{d\psi_d}{dt} \tag{40}$$

$$\psi_d(t) = \psi_d(0) + \int_0^t \left(u_d(\tau) - Ri_d(\tau)\right) d\tau \tag{41}$$

If the resistance R and the time behaviours of u_d and i_d are known, the time behaviour of ψ_d can be determined by (41), where $\psi_d(0)$ is the flux linkage due to the remanent flux. Fig. 4 shows the applied stepwise changing voltage $u_d(t)$ and the responding current $i_d(t)$ measured during the test.

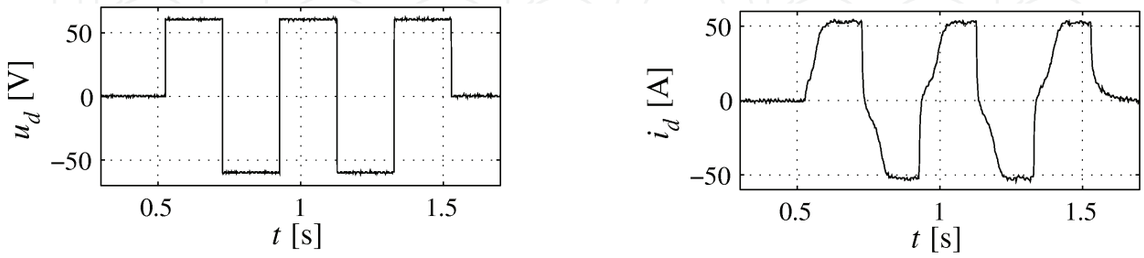

Fig. 4. Applied stepwise changing voltage $u_d(t)$ and responding current $i_d(t)$

The calculated time behaviour of the flux linkage $\psi_d(t)$ is shown in Fig. 5a. Fig. 5b shows the flux linkage $\psi_d(t)$ presented as a function of $i_d(t)$ in the form of a hysteresis loop $\psi_d(i_d)$. By calculating the average value of the currents for each flux linkage value, the unique characteristic $\psi_d(i_d)$, shown in Fig. 5c, is determined. The unique characteristic $\psi_d(i_d)$ shown in Fig. 5d is obtained by mapping the part of the characteristic $\psi_d(i_d)$, shown in Fig. 5c, from the third quadrant into the first quadrant and by calculating the average value of the currents for each value of the flux linkages again. By repeating the described procedure for different and equidistant values of the closed-loop controlled currents in both axes, the characteristics $\psi_d(i_d,i_q)$ and $\psi_q(i_d,i_q)$ can be determined for the given position x. To determine

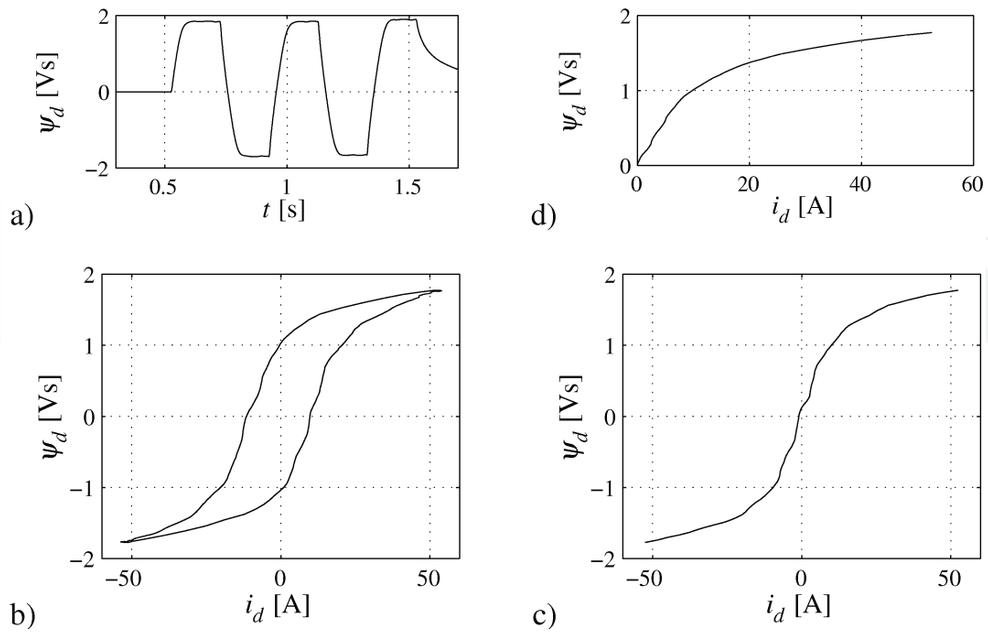

Fig. 5. Flux linkage time behaviour $\psi_d(t)$ a); hysteresis loop $\psi_d(i_d)$ b); unique characteristic $\psi_d(i_d)$ in the first and third quadrant c); unique characteristic $\psi_d(i_d)$ in the first quadrant d)

the current and position dependent characteristics $\psi_d(i_d,i_q,x)$ and $\psi_q(i_d,i_q,x)$, the tests must be repeated for different equidistant positions of the locked mover over at least one pole pitch. During the tests, the magnitude of the stepwise changing voltage should be high enough to assure that the responding current covers the entire range of operation. The frequency of the applied voltage must be low enough to allow the current to reach the steady-state before the next change. Since the expression (41) represents an open integrator without any feedback, the obtained results are extremely sensitive to the incorrect values of the resistance R. The steady-state values of the voltage and current can be used to calculate the resistance R after each voltage step change. The voltages generated by an inverter are normally pulse width modulated, whereas the measurement of such voltages could be a demanding task. The method for determining characteristics of flux linkages presented in this subsection gives acceptable results even when the voltage reference values are used instead of the measured ones. However, calculation of the resistance value after each voltage step change is substantial. Some of the methods that can be also applied for determining the magnetically nonlinear characteristics of magnetic cores inside electromagnetic devices and electric machines are presented in (Štumberger, 2005, 2008).

3.3 Thrust and friction force

The experimental setup shown in Fig. 3 is applied to determine the thrust F_e and the friction force F_f. The d-axis current and the q-axis current are closed-loop controlled in order to keep the preset constant values. The external source of force, in the form of a driving motor, is applied to move the mover of the LSRM at the constant speed of 0.02 m/s over two pole pitches from left to right and back again. The force causing the motion of the mover is measured by a force sensor. Since the friction force always opposes the force causing motion, one half of the difference between the forces measured for the moving left and right is the friction force, while the average value of both measured forces is the thrust. Fig. 6 shows the position dependent forces measured for the moving left and right together with the thrust and friction force. They are given over two pole pitches. To determine the thrust and friction force characteristics over the entire range of operation, the tests are repeated for different preset constant values of the closed-loop controlled currents in the axes d and q.

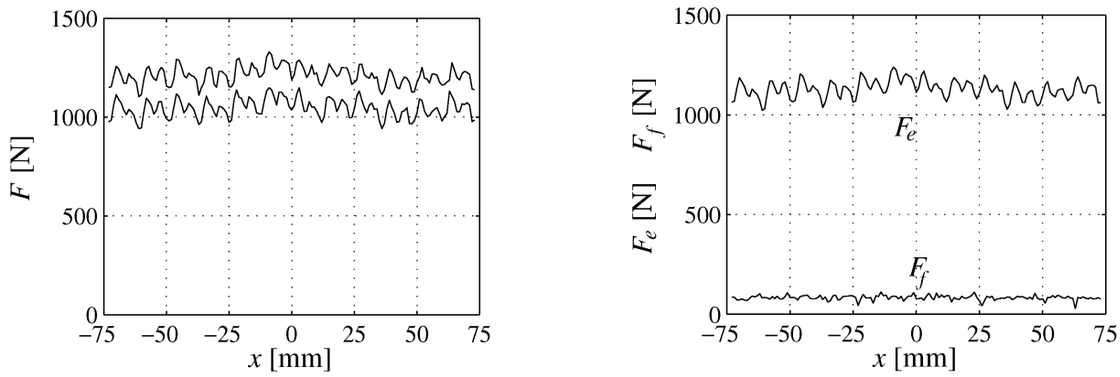

Fig. 6. Force F measured for moving left and right, thrust F_e and friction force F_f.

4. Results

The magnetically nonlinear dynamic models of permanent magnet and reluctance synchronous machines are presented in the section 2. These models are of no use without

their parameters, given in the form of current and position dependent characteristics of flux linkages. Some of the methods, appropriate for determining these parameters are presented in the section 3. This section focuses on the linear synchronous reluctance motor. The characteristics of flux linkages, thrust and friction force, determined by the methods described in section 3, are presented. Applications of the proposed models are shown at the end of this section.

Figs. 7 and 8 show the characteristics of flux linkages $\psi_d(i_d,i_q,x)$ and $\psi_q(i_d,i_q,x)$. They are determined over the entire range of operation using the method presented in the subsection 3.2. Fig. 9 and 10 show the thrust characteristics determined by the method described in the subsection 3.3.

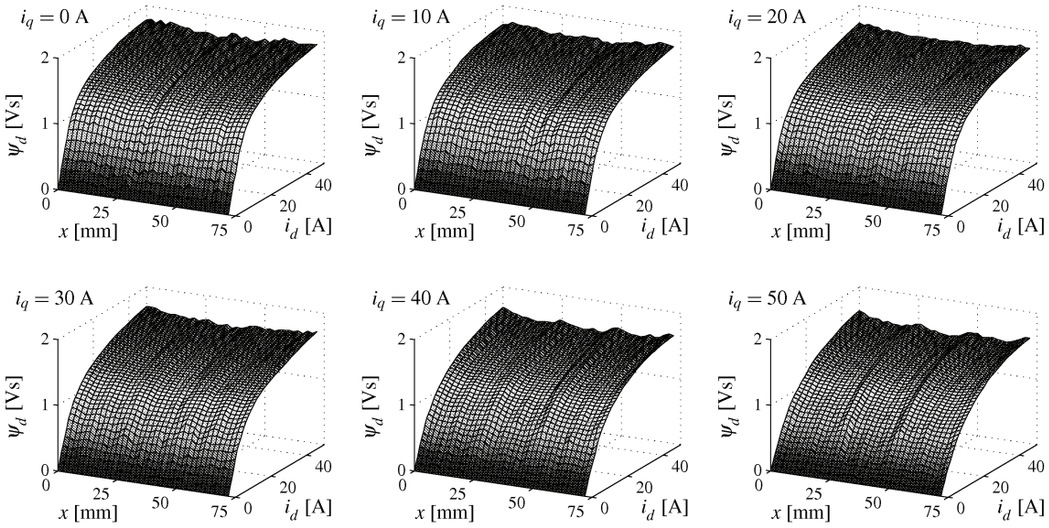

Fig. 7. Characteristics $\psi_d(i_d,i_q,x)$ given over one pole pitch for different constant values of current i_q

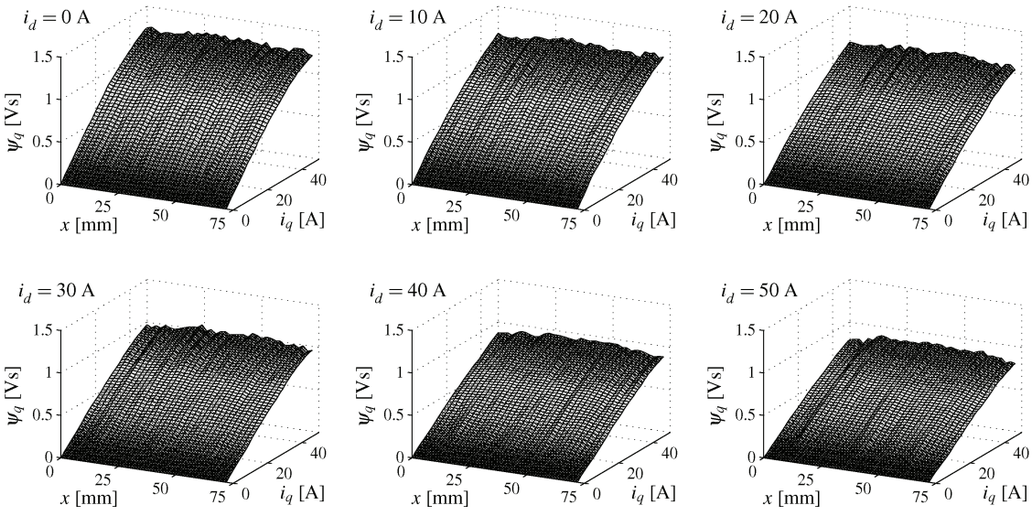

Fig. 8. Characteristics $\psi_q(i_d,i_q,x)$ given over one pole pitch for different constant values of current i_d

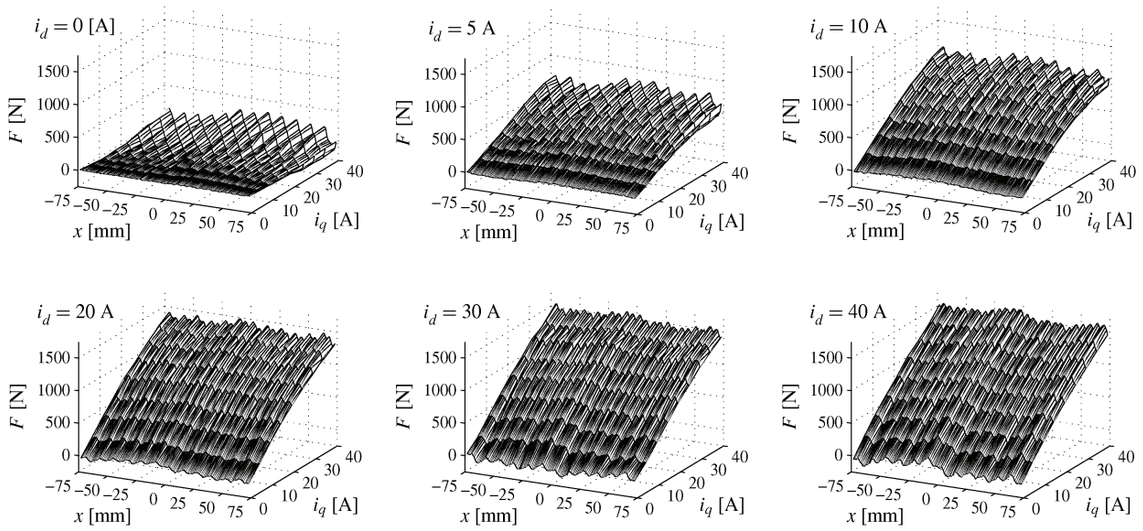

Fig. 9. Characteristics $F_e(i_d,i_q,x)$ given over two pole pitches for different constant values of current i_d

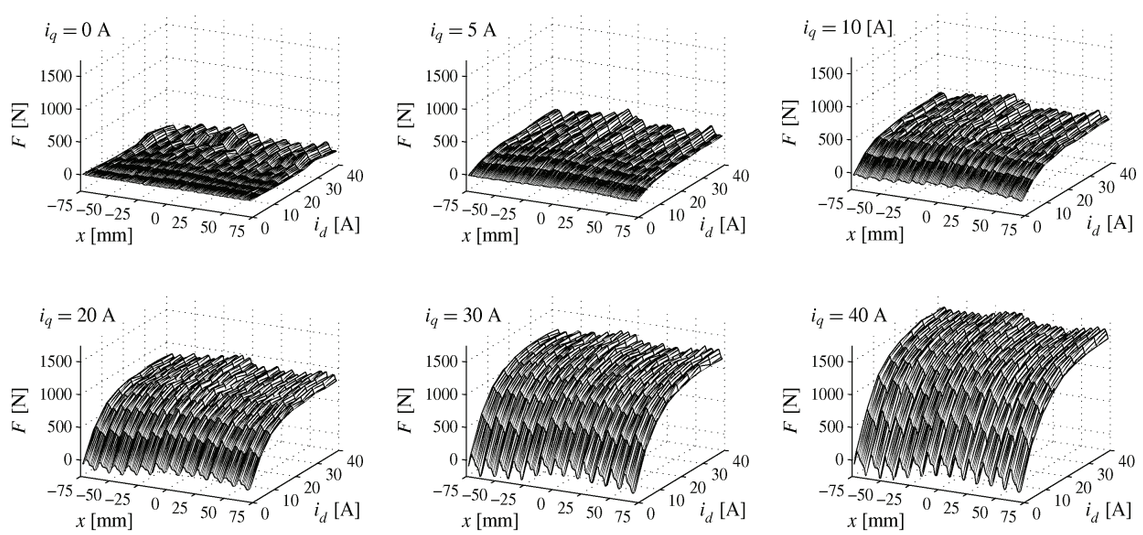

Fig. 10. Characteristics $F_e(i_d,i_q,x)$ given over two pole pitches for different constant values of current i_q

Figs. 11 to 14 show the trajectories of individual variables for the case of a kinematic control performed with experimental setup shown in Fig. 3. Figs. 11 and 12 give results for the kinematic control performed at higher speed, whereas the results presented in Figs. 13 and 14 are given for the kinematic control performed at much lower speed. Figs. 11 and 13 show the trajectories of the position x and current i_d measured during the experiment. These trajectories are used in the model to calculate the corresponding trajectories of the speed v and current i_q. The measured and calculated trajectories are shown in Figs. 12 and 14. The calculations are performed with the dynamic model of the LSRM given by equations (21) to (29), considering characteristics of flux linkages given in Figs. 7 and 8.

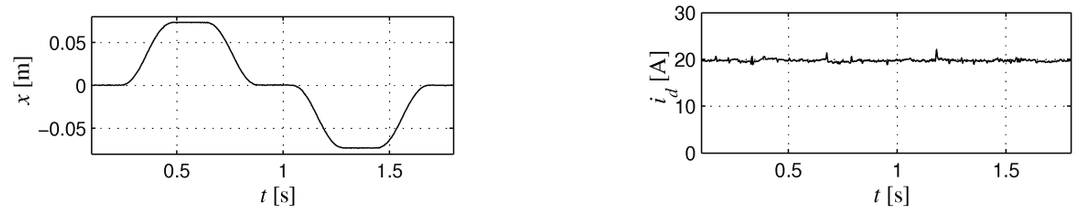

Fig. 11. Trajectories of position x and current i_d measured on the experimental system in the case of kinematic control

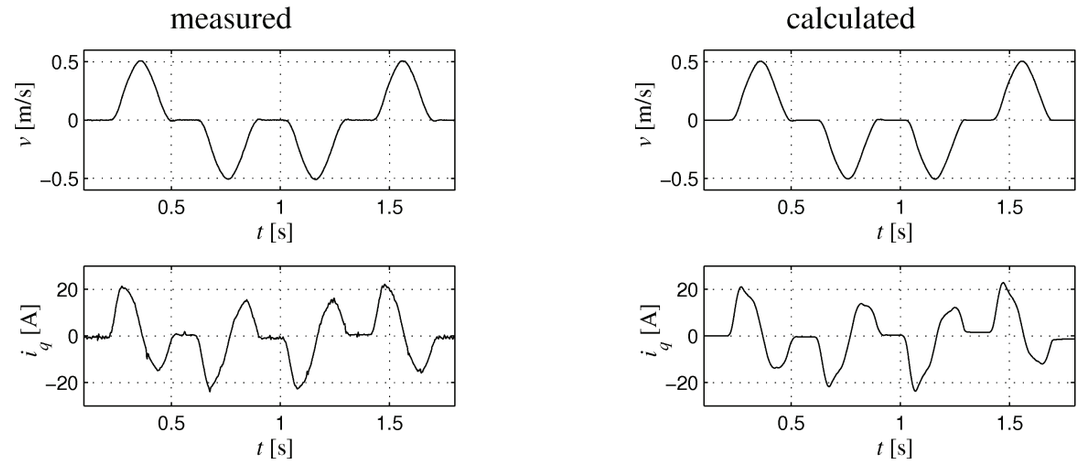

Fig. 12. Measured and calculated trajectories of speed $v=dx/dt$ and current i_q in the case of kinematic control with position trajectory given in Fig. 11

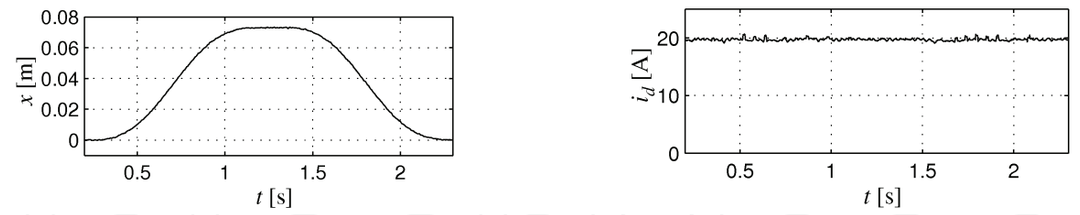

Fig. 13. Trajectories of position x and current i_d measured on the experimental system in the case of low speed kinematic control

The results presented in Fig. 14 clearly show that the measured as well as the calculated speed trajectories are deteriorated due to the effects of slotting. The mass of the mover filters these effects out at higher speeds, as shown in Fig. 12.

The results presented in Fig. 14 show that the magnetically nonlinear dynamic models of synchronous machines presented in this chapter contain the effects of slotting. In the next example, the models are involved in the design of nonlinear control with input-output decoupling and linearization described in (Dolinar, 2005). Fig. 15 shows the results of experiments performed on the experimental setup shown in Fig. 3. Compared are the results of low speed kinematic control obtained with two different control realizations. In the first realization, the control design is based on the magnetically linear model of tested linear synchronous reluctance machine. In the second one, the control design is based on the

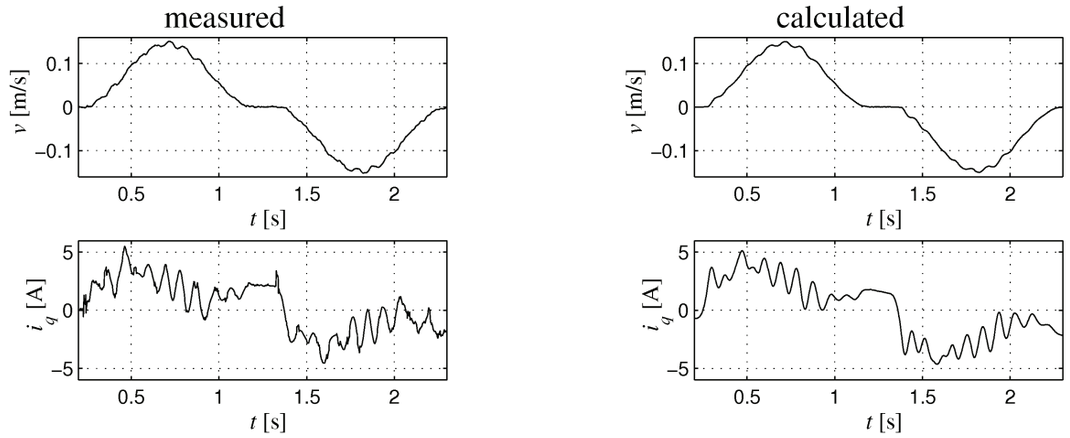

Fig. 14. Measured and calculated trajectories of speed $v=dx/dt$ and current i_q in the case of low speed kinematic control with position trajectory given in Fig. 13

magnetically nonlinear model presented in this work. Fig. 15 compares the trajectories of position reference, position, position error, speed reference, speed, speed error, d- and q-axis currents, and d- and q-axis voltages for both control realizations. The results presented in Fig. 15 clearly show a substantial improvement of the low speed kinematic control performance in the case when the magnetically nonlinear dynamic model is applied in the nonlinear control design. The position error is reduced for more than five times while the speed error is reduced for more than two times. However, as it is shown in Figs. 11 to 14, the magnetically nonlinear dynamic models presented in this chapter can substantially contribute to the position error reduction at very low speeds, whereas at higher speeds the mass of the mover filter these effects out.

5. Conclusion

This chapter deals with the magnetically nonlinear dynamic models of synchronous machines. The procedure that can be used to derive the magnetically nonlinear dynamic model of synchronous machines is presented in the case of rotational permanent magnet synchronous machine. The obtained model is then modified in order to be suitable for description of the rotary and linear synchronous reluctance machine. Since the model is useless without its parameters, the experimental methods suitable for determining model parameters are described. They are presented in the form of current and position dependent characteristics of flux linkages, given for the tested linear synchronous reluctance machine. The effects of slotting, saturation, cross-saturation, and end effects are accounted for in the models. The models can help to reduce the tracking errors when used in the control design.

6. References

Abdallh, A.A.E.; Sergeant, P.; Crevecoeur, G.; Vandenbossche, L.; Dupre, L. & Sablik, M. (2009). Magnetic Material Identification in Geometries with Non-Uniform Electromagnetic Fields Using Global and Local Magnetic Measurements. *IEEE Transactions on Magnetics,* Vol. 45, No. 10, November 2009 page numbers 4157-4160, ISSN: 0018-9464

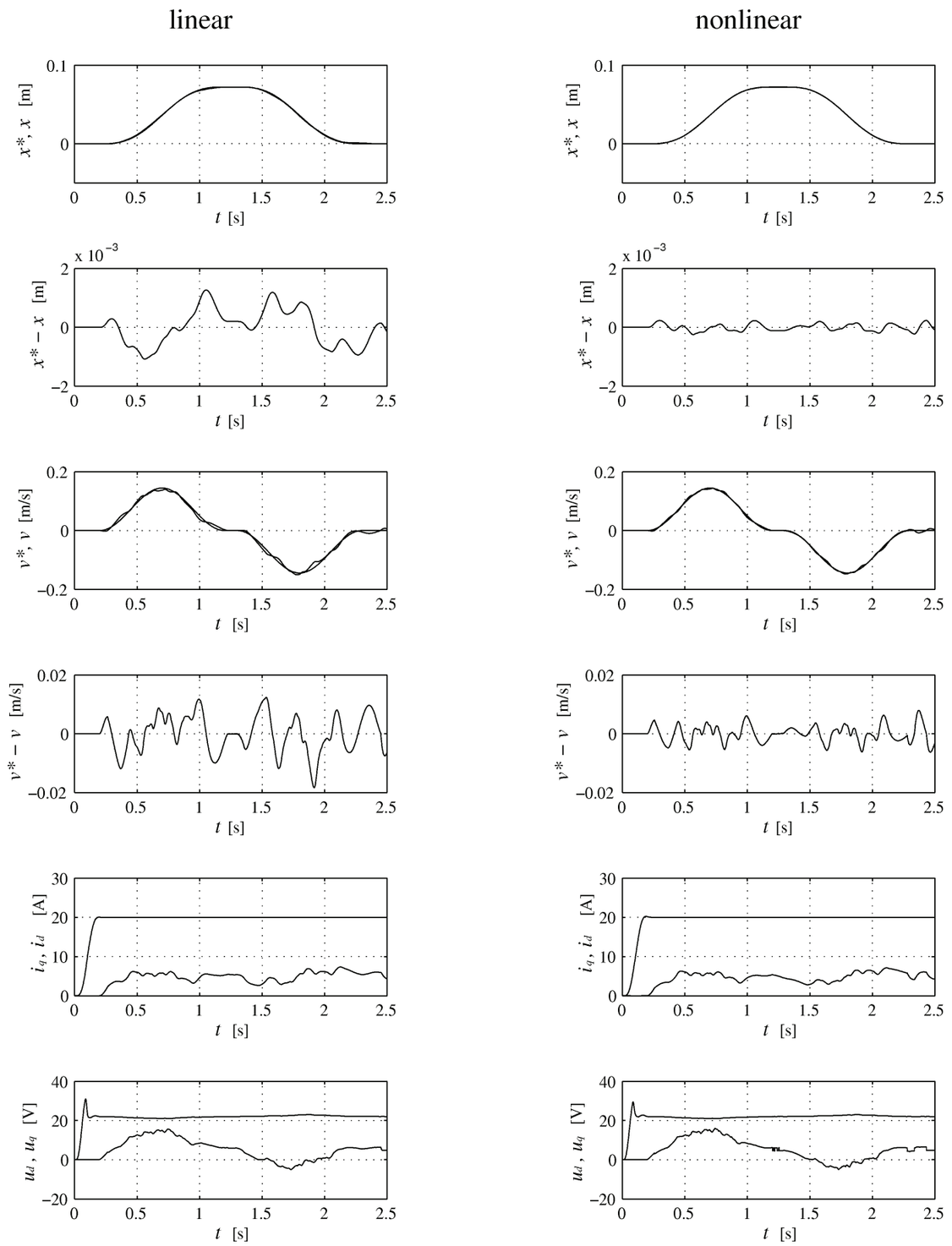

Fig. 15. Trajectories of position x and position reference x^*, position error x^*-x, speed v and speed reference v^*, speed error v^*-v, currents i_d and i_q, and voltages u_d and u_q measured on experimental setup for the cases when the linear and nonlinear LSRM dynamic models are applied in the control design

Boldea, I. & Tutelea, L. (2010). *Electric machines: steady states, transients, and design with Matlab,* CRC Press, ISBN: 978-1-4200-5572-6, New York

Boll, R. (1990). *Weichmagnetische Werkstoffe,* Vakuumschmelze GmbH, Hanau

Capecchi, E.; Guglielmi, P.; Pastorelli, M. & Vagati, A. (2001). Position-sensorless control of the transverse-laminated synchronous reluctance motor. *IEEE Transactions on Industry Applications,* Vol. 37, No. 6, November/December 2001 page numbers 1768-1776, ISSN: 0093-9994

Daldaban, F. & Ustkoyuncu, N. (2006). A new double sided linear switched reluctance motor with low cost. *Energy Conversion and Management,* Vol. 47, No. 18-19, November 2006 page numbers 2983-2990, ISSN: 0196-8904

Daldaban, F. & Ustkoyuncu, N. (2007). New disc type switched reluctance motor for high torque density. *Energy Conversion and Management,* Vol. 48, No. 8, August 2007 page numbers 2424-2431, ISSN: 0196-8904

Daldaban, F. & Ustkoyuncu, N. (2010). A novel linear switched reluctance motor for railway transportation systems. *Energy Conversion and Management,* Vol. 48, No. 8, March 2010 page numbers 465-469, ISSN: 0196-8904

Dolinar, D; Ljušev, P. & Štumberger, G. (2003). Input-output linearising tracking control of an induction motor including magnetic saturation effects. *IEE Proceedings – Electric Power Applications,* Vol. 150, Issue 6, November 2003 page numbers 703-711, ISSN: 1350-1352

Dolinar, D; Štumberger, G. & Milanovič, M. (2005). Tracking improvement of LSRM at low-speed operation. *European Transactions on Electrical Power,* Vol. 15, Issue 3, May/June 2005 page numbers 257-270, ISSN: 1430-144X

Dolinar, D. & Štumberger, G. (2006). *Modeliranje in vodenje elektromehanskih sistemov,* Založniška dejavnost FERI, ISBN: 86-435-0672-9, Maribor

Fitzgerald, A. E. & Kingslley., C. Jr. (1961). *Electric machinery,* McGraw-Hill Book Company, New York

Guglielmi, P.; Pastorelli, M. & Vagati, A. (2006). Impact of cross-saturation in sensorless control of transverse-laminated synchronous reluctance motors. *IEEE Transactions on Industrial Electronics,* Vol. 53, No. 2, April 2006 page numbers 429-439, ISSN: 0278-0046

Hadžiselimović, M. (2007a). *Magnetically nonlinear dynamic model of a permanent magnet synchronous motor,* Ph.D. Thesis, University of Maribor, Maribor

Hadžiselimović, M.; Štumberger, G.; Štumberger, B. & Zagradišnik, I. (2007b). Magnetically nonlinear dynamic model of synchronous motor with permanent magnets. *Journal of Magnetism and Magnetic Materials,* Vol. 316, Issue 2, 2007 page numbers e257-e260, ISSN: 0304-8853

Hadžiselimović, M.; Štumberger, B.; Virtič, P.; Marčič, T. & Štumberger, G. (2008). Determining parameters of a two-axis permanent magnet synchronous motor dynamic model by finite element method. *Przegląd Elektrotechniczny,* Vol. 84, No. 1, 2008 page numbers 77-80, ISSN: 0033-2097

Hamler, A.; Trlep, M. & Hribernik, B. (1998). Optimal secondary segment shapes of linear reluctance motors using stochastic searching. *IEEE Transactions on Magnetics,* Vol. 34, No. 5, September 1998 page numbers 3519-3521, ISSN: 0018-9464

Iglesias, I.; Garcia-Tabares, L. & Tamarit, J. (1992). A d-q model for the self-commutated synchronous machine considering magnetic saturation. *IEEE Transactions on Energy Conversion,* Vol. 7, No. 4, December 1992 page numbers 768-776, ISSN: 0885-8969

Jadrić, M.; & Frančić, B. (1997). *Dinamika električnih strojeva,* Sveučilište u Splitu, ISBN: 953-96399-2-1, Split

Krause, P. C.; Wasynczuk, O. & Sudhoff, S. D. (2002). *Analysis of electric machinery,* IEEE Press, ISBN: 0-471-14326-X, New York

Kron, G. (1951). *Equivalent circuits of electric machinery,* J. Wiley & Sons, New York

Kron, G. (1959). *Tensor for circuits,* Dover, New York

Kron, G. (1965). *Tensor analysis of networks,* MacDonald, London

Levi, E. & Levi, V. A. (2000). Impact of dynamic cross-saturation on accuracy of saturated synchronous machine models. *IEEE Transactions on Energy Conversion,* Vol. 15, No. 2, June 2000 page numbers 224-230, ISSN: 0885-8969

Marčič, T.; Štumberger, G.; Štumberger, B.; Hadžiselimović, M. & Virtič, P. (2008). Determining parameters of a line-start interior permanent magnet synchronous motor model by the differential evolution. *IEEE Transactions on Magnetics,* Vol. 44, No. 11, November 2008 page numbers 4385-4388, ISSN: 0018-9464

Melkebeek, J. A. & Willems, J. L. (1990). Reciprocity relations for the mutual inductances between orthogonal axis windings in saturated salinet-pole machines. *IEEE Transactions on Industry Applications,* Vol. 26, No. 1, January/February 1990 page numbers 107-114, ISSN: 0093-9994

Owen, E. L. (1999). History: Charles Concodia 1999 IEEE Medal of Honor. *IEEE Industry Applications Magazine,* Vol. 5, No. 3, May/June 1999 page numbers 10-16, ISSN: 1077-2618

Rahman, K.A. & Hiti, S. (2005). Identification of machine parameters of a synchronous motor. *IEEE Transactions on Industry Applications,* Vol. 41, No. 2, March/April 2005 page numbers 557-567, ISSN: 0093-9994

Sauer, P. W. (1992). Constraints on saturation modeling in ac machines. *IEEE Transactions on Energy Conversion,* Vol. 7, No. 4, March 1992 page numbers 161-167, ISSN: 0885-8969

Štumberger, B.; Štumberger, G.; Dolinar, D.; Hamler, A. & Trlep, M. (2003). Evaluation of saturation and cross-magnetization effects in interior permanent-magnet synchronous motor. *IEEE Transactions on Industry Applications,* Vol. 39, No. 5, September/October 2003 page numbers 1265-1271, ISSN: 0093-9994

Štumberger, G.; Štumberger, B. & Dolinar, D. (2003). Magnetically nonlinear and anisotropic iron core model of synchronous reluctance motor. *Journal of Magnetism and Magnetic Materials,* Vols. 254/255, No. 1, January 2003 page numbers 618-620, ISSN: 0304-8853

Štumberger, G.; Štumberger, B.; Dolinar, D. & Težak, O. (2004a). Nonlinear model of linear synchronous reluctance motor for real time applications. *Compel,* Vol. 23, No. 1, 2004 page numbers 316-327, ISSN: 0332-1649

Štumberger, G.; Štumberger, B. & Dolinar, D. (2004b). Identification of linear synchronous reluctance motor parameters. *IEEE Transactions on Industry Applications,* Vol. 40, No. 5, September/October 2004 page numbers 1317-1324, ISSN: 0093-9994

Štumberger, G.; Polajžer, B.; Štumberger, B. & Dolinar, D. (2005). Evaluation of experimental methods for determining the magnetically nonlinear characteristics of

electromagnetic devices. *IEEE Transactions on Magnetics,* Vol. 41, No. 10, October 2005 page numbers 4030-4032, ISSN: 0018-9464

Štumberger, G.; Štumberger, B. & Dolinar, D. (2006). Dynamic two-axis model of a linear synchronous reluctance motor based on current and position-dependent characteristics of flux linkages. *Journal of Magnetism and Magnetic Materials,* Vol. 304, No. 2, 2006 page numbers e832-e834, ISSN: 0304-8853

Štumberger, G.; Seme, S.; Štumberger, B.; Polajžer, B. & Dolinar, D. (2008a). Determining magnetically nonlinear characteristics of transformers and iron core inductors by differential evolution. *IEEE Transactions on Magnetics,* Vol. 44, No. 6, June 2008 page numbers 1570-1573, ISSN: 0018-9464

Štumberger, G.; Marčič, T.; Štumberger, B. & Dolinar, D. (2008b). Experimental method for determining magnetically nonlinear characteristics of electric machines with magnetically nonlinear and anisotropic iron core, damping windings, and permanent magnets. *IEEE Transactions on Magnetics,* Vol. 44, No. 11, November 2008 page numbers 4341-4344, ISSN: 0018-9464

Tahan, S. A. & Kamwa, I. (1995). Two-factor saturation model for synchronous machines with multiple rotor circuits. *IEEE Transactions on Energy Conversion,* Vol. 10, No. 4, December 1995 page numbers 609-616, ISSN: 0885-8969

Vas, P.; Hallenius, K. E. & Brown, J. E. (1986). Cross-saturation in smooth-air-gap electrical machines. *IEEE Transactions on Energy Conversion,* Vol. 1, No. 1, March 1986 page numbers 103-112, ISSN: 0885-8969

Vas, P. (1992). *Electrical machines and drives,* Clarendon Press, ISBN: 0-19-859378-3, Oxford

Vas, P. (2001). *Sensorless Vector and Direct Torque Control,* Oxford University Press, ISBN: 978-0-19-856465-1, New York

Vagati, A.; Pastorelli, M.; Scapino, F. & Franceschini, G. (2000). Impact of cross saturation in synchronous reluctance motors of the transverse-laminated type. *IEEE Transactions on Industry Applications,* Vol. 36, No. 4, July/August 2000 page numbers 1039-1046, ISSN: 0093-9994

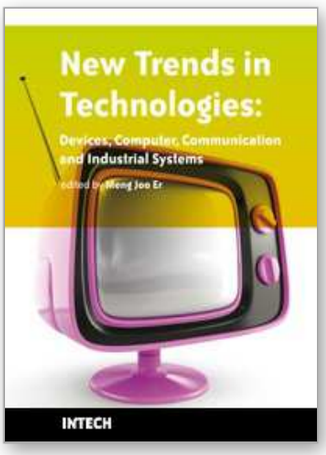

New Trends in Technologies: Devices, Computer, Communication and Industrial Systems
Edited by Meng Joo Er

ISBN 978-953-307-212-8
Hard cover, 444 pages
Publisher Sciyo
Published online 02, November, 2010
Published in print edition November, 2010

The grandest accomplishments of engineering took place in the twentieth century. The widespread development and distribution of electricity and clean water, automobiles and airplanes, radio and television, spacecraft and lasers, antibiotics and medical imaging, computers and the Internet are just some of the highlights from a century in which engineering revolutionized and improved virtually every aspect of human life. In this book, the authors provide a glimpse of new trends in technologies pertaining to devices, computers, communications and industrial systems.

How to reference
In order to correctly reference this scholarly work, feel free to copy and paste the following:

Gorazd Štumberger, Bojan Štumberger, Tine Marčič, Miralem Hadžiselimović and Drago Dolinar (2010). Magnetically Nonlinear Dynamic Models of Synchronous Machines: Their Derivation, Parameters and Applications, New Trends in Technologies: Devices, Computer, Communication and Industrial Systems, Meng Joo Er (Ed.), ISBN: 978-953-307-212-8, InTech, Available from: http://www.intechopen.com/books/new-trends-in-technologies--devices--computer--communication-and-industrial-systems/magnetically-nonlinear-dynamic-models-of-synchronous-machines-their-derivation-parameters-and-applic

INTECH
open science | open minds

InTech Europe
University Campus STeP Ri
Slavka Krautzeka 83/A
51000 Rijeka, Croatia
Phone: +385 (51) 770 447
Fax: +385 (51) 686 166
www.intechopen.com

InTech China
Unit 405, Office Block, Hotel Equatorial Shanghai
No.65, Yan An Road (West), Shanghai, 200040, China
中国上海市延安西路65号上海国际贵都大饭店办公楼405单元
Phone: +86-21-62489820
Fax: +86-21-62489821

IntechOpen